BACCHUS : an Aero-Acoustic Test Bench oriented towards Microphone Assembly and De-Noising Method Development

Jeremie Derre, Olivier Sainges

BACCHUS : AN AERO-ACOUSTIC TEST BENCH ORIENTED TOWARDS MICROPHONE ASSEMBLY AND DE-NOISING METHOD DEVELOPMENT

Jérémie Derré[1] **Olivier Saingès**[1]
[1] Acoustic Testing, Airbus, 316 route de Bayonne, 31060 Toulouse, France
jeremie.derre@airbus.com, olivier.o.sainges@airbus.com

ABSTRACT

This paper presents the development and validation of an aero-acoustic lab test rig, with some experimental results and findings coming from the first campaigns. This BACCHUS (Bench for ACoustic CHaracterization and Upgrade of Sensor) bench has been developed to investigate microphone mountings and processing de-noising methods, oriented towards in boundary layer investigations. The first part of this paper details some key elements of the bench development and validation, beginning with the vein anechoicity characterization, using temporal cross correlation analysis. Then, the velocity and Mach number evaluations are presented, with the velocity profiles. Additionally, a synchronous averaging processing method has been deployed and is presented, improving the signal to noise ratio, and resulting in a better acoustic emergence compared to the aerodynamics noise. In the second part, some experimental results are presented, starting with the turbulent boundary layer (TBL) noise assessment within a cavity.Finally, two campaign results are proposed, the first investigating the impact of the cavity cone angle regarding the TBL noise, and the second study evaluating the impact of the Mach number of the directivity of two microphones mountings.

1. INTRODUCTION

The acoustic measurement in an aerodynamic environment has been a challenging topic for researchers since several decades. Moreover, for aircraft manufacturer engineers, it has been even tougher to apply the lab-developed strategies in their industrial environment, flying aircraft. Indeed, the flight conditions are quite extreme (the temperature and the Mach for instance), especially because they could strongly vary during a single flight path.
Therefore, the need to develop and characterize smart methods is key, combining microphone assembly and post-processing algorithm. The BACCHUS (Bench for ACoustic CHaracterization and Upgrade of Sensor) bench has been developed in such a frame, for aero-acoustic applications. To be more precise, the scope is linked to external aircraft acoustic measurement issues, as being most of the time wall mounted sensors on the aircraft fuselage, and therefore immersed in the flow and the boundary layer. The bench allows to develop, test, and validate method efficiency with limited resources in a lab environment, before larger deployment, such as large wind tunnel testing and finally aircraft flight test campaigns. This research field keeps growing, as the noise reduction targets continuously decrease, especially to reduce the annoyance in more and more crowded areas around airports. Some studies focus on wall treatment of the wind tunnel vein [1], and other on different microphones assemblies [2–4], as well as advanced postprocessing methods [5].

The specificity of the BACCHUS bench is that it is dedicated to the instrumentation and method development [6, 7], rather than being a wind tunnel used to characterize systems (wing profile, aircraft scale model, landing gear, etc.) with given acoustic techniques, which can latter can be optimized for the item to be measured. This bench could be used in three different ways : with the flow only to investigate TBL noise, with the acoustics only to assess directivity without the flow effect, and both with the flow and the acoustic generation, leading to full aero-aoustic measurement.

This paper is organized in two main parts. The first one introduces some of the key elements of the bench development and characterization, starting with a general presentation of the test mean. Then, the vein anechoicity characterization is detailed, using temporal cross correlation analysis, in order to investigate the reflected waves and their contribution. Afterwards, the velocity and Mach number evaluations are introduced, with the velocity profiles which are found coherent compared to expectations in such a bench. Finally, the bench uses a synchronous averaging processing method, improving the signal to noise ratio, and resulting in a better acoustic emergence compared to the aerodynamics noise.
The second part presents some experimental results, starting with the turbulent boundary layer (TBL) noise assessment within a cavity and recessed microphone, that shows the noise decreasing with the increasing depth of the sensor at several frequencies. Then, the first investigations of the impact of the cavity cone angle regarding the TBL noise are discussed. Finally, a second study aiming at evaluating the impact of the Mach number of the directivity of two microphones mountings is detailed, enlightening the convection effects due to the Mach.
Another study [8] presents a comparison of some experimental results measured on the BACCHUS bench and a numerical study conducted in parallel.

2. BENCH DEVELOPMENT AND CHARACTERIZATION

2.1 General bench presentation

Fig. 1 proposes three views of the bench. The anechoic central section is about 2m long, flanked by two tranquilization sections of 2m each, before the upstream convergent and the downstream divergent sections. An overview of the whole bench could be found in Fig. 9, with the purpose of showing the aerodynamic sensor positions. With a

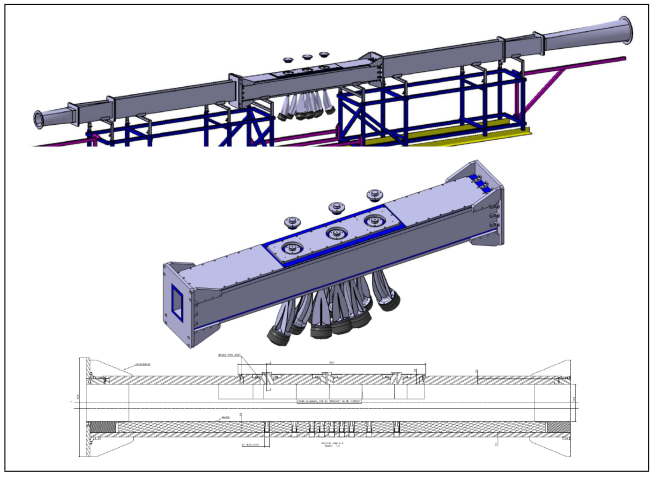

Figure 1. Sketch (up) of the whole bench, and (down) two images of the measurement section (nothing at scale).

rectangular section of 110mm per 70mm, three of the sides are covered with 50mm acoustic melamine foam, considered as non-reflective in the frequency range of interest, as shown later in this paper. The last wall allows to insert different rigid structures, which contain the microphone assembly of interest, over a 1m-long opening. Facing the microphones, a set of nine acoustic sources is embedded in the foam, each consisting in a compression driver mounted with a convergent trump, finished with an acoustic mesh. Twelve 1/4 inch pressure field microphones are used, nine in the nine horns to monitor the generated acoustic levels, three to be tested in the three measurement positions. The measurement vein, terminated at both ends with tranquilization sections and their convergent/divergent ducts, is coupled with a high capacity air supplier, which allows to reach Mach 0.55 in the vein center.
This bench has, among other applications, been developed to measure the microphone assembly angular directivity. The excitation configuration allows to test aperture angle of the assembly from 30 degrees up to 150 degrees.

2.2 Anechoicity characterization

In order to assess the bench anechoicity, an investigation based on temporal correlation analysis has been performed. Generally speaking, the cross-correlation evaluates the similarity of a time signal with another signal shifted in time. It grows towards its maximum (0 in a log-scale) at timeshift where the two signals are more likely similar. The auto-correlation (or sometimes self-correlation) might help to identify the presence of reflections in a given recorded signal, as well as to quantify its level and the echo time delay. In Fig. 2, a rigid plate has been mounted into the bench vein, at a known position. With the temperature information, the flight time

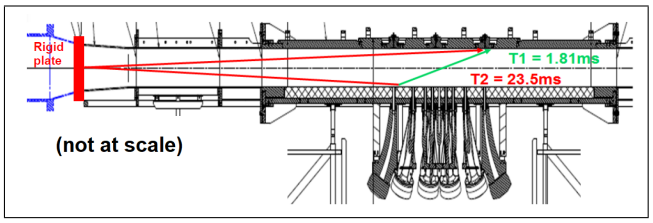

Figure 2. Sketch of the bench with a rigid plate mounted on (not at scale).

of an acoustic wave pulse can be easily evaluated without flow. Such procedure has been performed with a random noise filtered in third octave bands, for all third octave bands in the range 0.5 up to 20 kHz, and that for all three microphones positions and the nine loudspeakers.

Fig. 3 plots the auto-correlation [9] of the microphone inserted in the first position with the ninth loudspeaker generating both with and without the rigid plate. The curve

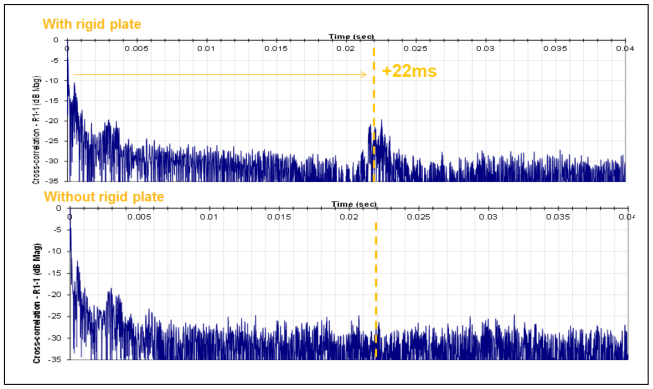

Figure 3. Auto-correlation of the microphone inserted in the first position with the ninth loudspeaker generating : with the rigid plate (up) and without (down).

with the rigid plate exhibits a significant reflection about 22ms. From Fig. 2, Δt_{21} the time delay between T_1 the direct ray between the loudspeaker and the microphone, and T_2 the direct ray from the reflection on the rigid plate is Eqn. (1)

$$\Delta t_{21} = T_2 - T_1 \simeq 21.7\text{ms}, \qquad (1)$$

which corresponds to what has been observed in Fig. 3.

If a closer look is given at the first part of this auto-correlation, two peaks can be observed in Fig. 4. The first peak is about 0.5 ms. In Fig. 5, the direct ray is sketched, as well as the second order ray, with its two reflections, firstly in the top hardwall, and secondly after crossing the foam. The flight time difference Δt_{31} is evaluated as Eqn. (2)

$$\Delta t_{31} = T_3 - T_1 = 2.34 - 1.81 = 0.53\text{ms}, \qquad (2)$$

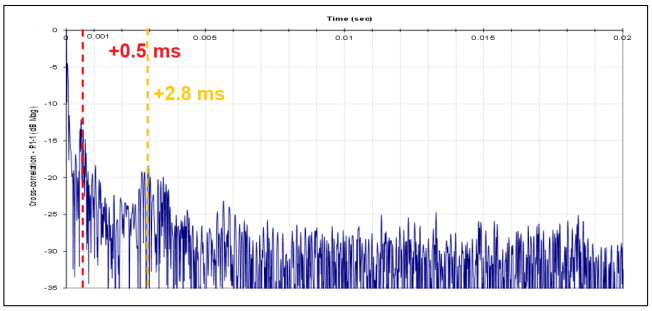

Figure 4. Auto-correlation of the microphone inserted in the first position with the ninth loudspeaker generating (zoom).

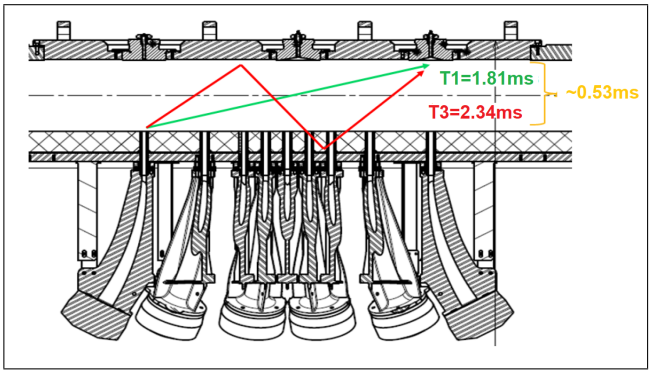

Figure 5. Sketch of the direct ray (green) and second order ray (red).

and corresponds to the first peak observed in Fig. 4.

For the second peak, around $\simeq$ 2.9 ms, the generation montage is suspected. Indeed, as the compression driver is mounted at the end of a convergent horn, there might exist some standing waves in the horn. By evaluating the average length of the horn from the compression driver to the bench as $L_{\text{horn}} \simeq 470$mm, the flight time of roundtrip is about Eqn. (3)

$$\Delta t_{\text{horn}} = \frac{2L_{\text{horn}}}{c_0} \simeq 2.8\text{ms}, \tag{3}$$

as shown in Fig. 6. This roundtrip might be linked to the acoustic energy reflected at the horn tip, travelling back to the compression driver, rebounding in it, and travelling back again to the horn tip, towards the bench vein.

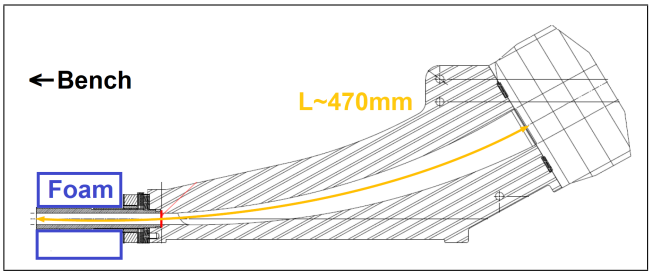

Figure 6. Sketch of the horn and compression driver.

As aforementioned, this study has been conducted with filtered random excitation, third octave band by third octave band, for every microphone and loudspeaker generation positions. Overall, it confirms that some reflections are still present in the bench, caused either by standing waves in the horns or the reflections within the vein, of pair orders. However, these non desirable reflected waves are quite less energetic than the direct incident ray, and could be easily identified. Therefore, the bench anechoicity is considered as validated in the third octave bands from 500Hz up to 20kHz.

2.3 Velocity and Mach number measurement

2.3.1 Mass flow measurement device

In order to measure Q_m the mass flow, a dedicated system have been developed and validated with calibrated mass flow meter up to 1kg.s^{-1}. It is composed of sixteen total pressure and sixteen static pressure measurements, distributed along two wing-shape profiles, as shown on Fig. 7. To calculate v the flow velocity and ρ the air density, a temperature probe and parietal static pressures are used. The mass flow Q_m is calculated as Eqn. (4)

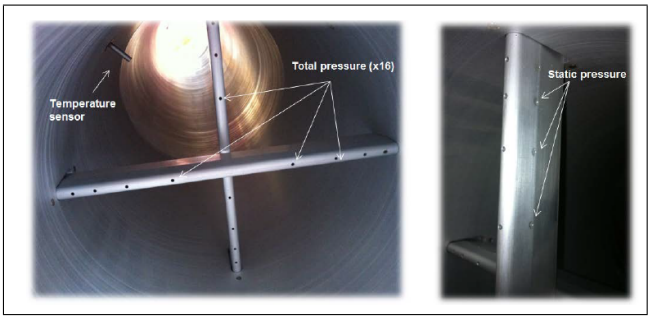

Figure 7. Pictures of some aerodynamic measurement devices.

$$Q_m = \rho\, v\, S\, C_d\,, \tag{4}$$

with C_d the pressure loss coefficient (a constant which depends on the flowmeter geometry). From Eqn. (4), the Mach number can therefore be calculated at this section of the vein, far enough from the measurement vein, in order not to modify the flow aerodynamic properties. Nevertheless, a dedicated validation test campaign has been performed, to validate this Mach measurement with the local Mach within the vein, as explained afterwards.

2.3.2 Mach number measurement validation

In order to characterize the velocity profiles and Mach numbers, scannings of the total pressure have been performed within the measurement vein. A Pitot comb tool has been designed and manufactured by the Airbus aerodynamic department, with nineteen orifices covering almost all the bench width, as shown on Fig. 8, with several pictures. In order to properly characterize the vertical direction of the bench cross-section, twenty-three positions have been scanned in the height, leading to a total of four

hundred thirty seven measurements. These measurements have been realized at the vein center (see the central anechoic section in Fig. 1 lower part), and for four Mach numbers : 0.12, 0.24, 0.37 and 0.53 .

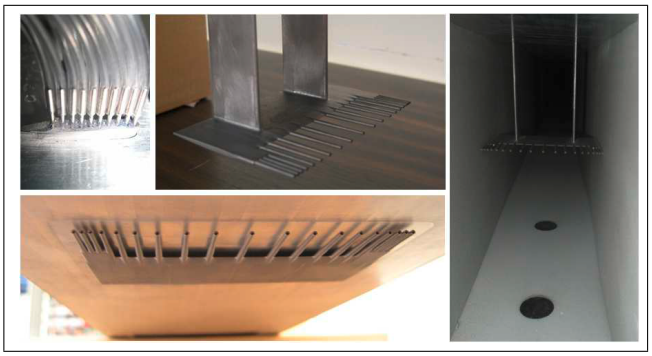

Figure 8. Pictures of the Pitot comb.

With the Pitot comb measuring the total pressure, two static pressure probes have been mounted as close as possible in the upstream and downstream tranquilizing sections, as sketched in Fig. 9. The static pressure at the Pitot comb position is interpolated from these two probes. Finally, the temperature is estimated from two sensors, one in the upstream exponential horn, the second in the mass flow section, as shown in Fig. 7.

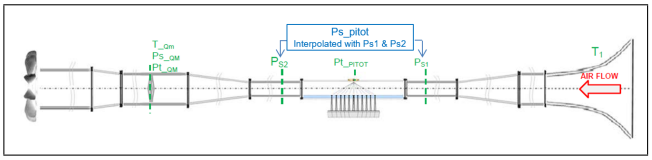

Figure 9. Sketch of the aerodynamic sensor positions.

Considering the air as a perfect gas, the air flow celerity v could be approximated such as follow.

• for Mach < 0.3, the flow is considered as incompressible. If the elevation term is neglected, the classical Bernoulli's equation [10] can be recast such as Eqn. (5)

$$\frac{\rho\, v^2}{2} + p_s = p_t, \tag{5}$$

with p_s and p_t the static and total pressures respectively. By using the perfect gas laws, this equation could be recast such as Eqn. (6), leading to $M = v/c$ the Mach number as

$$M = \left(2 \times \frac{p_t/p_s - 1}{\gamma}\right)^{1/2}, \tag{6}$$

with γ the Laplace's coefficient, and c the speed of sound.

• for Mach numbers in $0.3 < M < 0.8$, the flow is considered subsonic and compressible. Therefore, the Barré de Saint-Venant formulation could be used [10]. By keep neglecting the elevation term, one can establish Eqn. (7)

$$\frac{p_t}{p_s} = \left(1 + \frac{\gamma - 1}{2} M^2\right)^{\frac{\gamma}{\gamma - 1}}. \tag{7}$$

Tab. 1 presents the comparison of the mass flows Q_m^1 measured with a calibrated industrial mass flow meter and Q_m^2 obtained with the instrumentation and methods presented previously in this paper, both in g/s. The discrepancies between the results are small enough to consider the developed measurement system and calculation method such as validated for the mass flow range of interest.

Q_m^1	311	411	517	623	775	1162	1255
Q_m^2	305	414	497	604	762	1170	1272
Δ (%)	1.8	0.6	3.9	3.0	1.7	0.7	1.7

Table 1. Comparison of measured and calculated mass flows.

2.3.3 Velocity profiles

Fig. 10 presents the velocity profiles in the Y-axis, the horizontal plane. A good symmetry is observed among the width, and the boundary layer effect is identified on each side of the vein. Fig. 11 presents the velocity profiles in the Z-axis, the vertical plane. A significant asymmetry is observed between the top and the bottom velocity speeds, linked with the difference of the boundary layers. Indeed, the bottom side is made of the same foam as the two lateral walls, a bulk material, whereas the top side is consisting in a aluminum rigid wall. The roughness difference causes significant discrepancies in the boundary layer viscous effects.

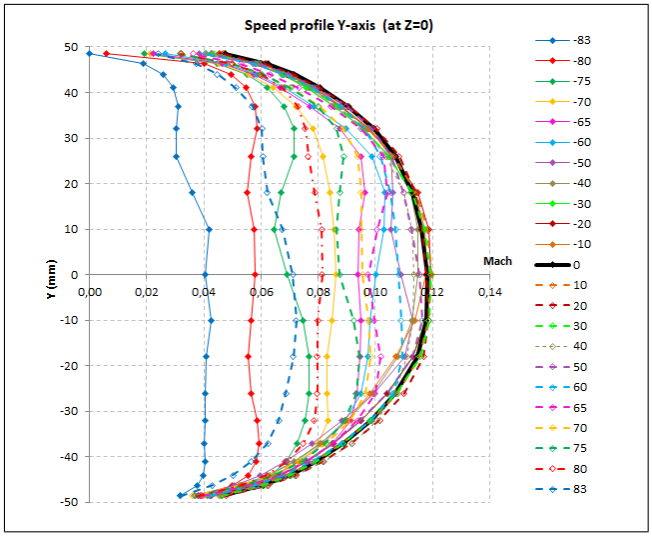

Figure 10. Velocity profile at Mach 0.12 in the Y-axis.

2.4 Synchronous averaging processing method

Due to the flow speed regimes, the noise within the vein is quite high, mainly due to the turbulent boundary layer (TBL). Therefore, it is rather difficult to get a controlled acoustic generation that is emerging from this TBL noise. Fig. 12 plots the spectrum of a 1/4 inch microphone mounted flush in the bench (solid blue line), as well as the

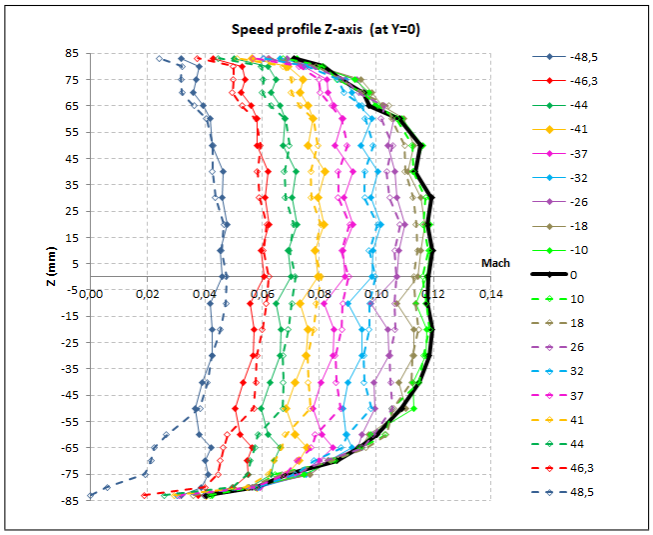

Figure 11. Velocity profile at Mach 0.12 in the Z-axis.

pure sine tones generated with different angular positions. The Tab. 2 presents the signal processing parameters used

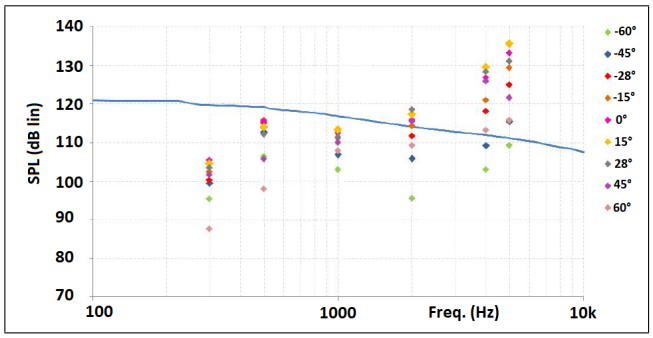

Figure 12. SPL of pure sine excitation for different angular position at Mach 0.45, the solid line (blue) being the flush microphone.

in this section. One could observe that below 2 kHz, most

Span	20 kHz
Lines	800
Δf	25 Hz
Window	Hann
Overlap	0 %

Table 2. Signal processing parameters.

of the tones do not emerge from the TBL noise, resulting in a "negative" signal to noise ratio (SNR).

If *a priori* knowledge of the under-investigation signal is accessible, and if the signal of interest is periodic, the use of time domain averaging allows to improve the SNR, by using synchronous averaging processing method [9] for instance. The founding idea is to use a trigger signal which is synchronous with the periodic signal of interest. This method is particularly relevant in the BACCHUS bench case because as being a relative approach, with the mounting of interest compared with the reference mounting (1/4 inch flush microphone without cavity and grid), most of the flow and vein installation effects are not taken into account, as being subtracted.

Fig. 13 plots the result of 1000 temporal windows used for averaging (about 40s recording time in this acquisition set-up), with the solid light blue curve as a result. It can be observed that compared to the other solid blue line, the SNR has been considerably improved, by about 30dB, and all the pure sine signals are now emerging from the background noise. The direct consequence is an expansion of the angular domain of interest, as well as a broader frequency range.

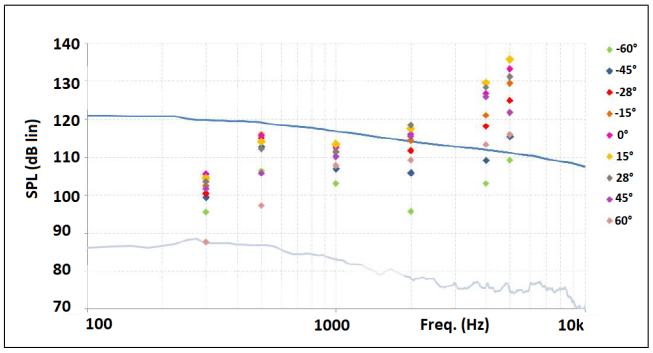

Figure 13. SPL of pure sine excitation for different angular position at Mach 0.45, and flush microphone after synchronous averaging processing on flush microphone (solid light blue line).

3. STUDIES AND ARRANGEMENT CHARACTERISATION

With this bench, several studies have already been carried out, such as the responses of different sensors under different wire meshes, the impact study of the mesh fiber alignment regarding the flow direction, or the sensor undermesh cavity with different geometries (depth and diameter) for instance. All these dedicated studies can be used afterwards as elementary bricks that provide guidelines to design the more proper solution to a given problematic. In this paper, a focus on three studies is proposed : the TBL noise reduction by retracting the sensor within the cavity depth, the impact of the cone angle and aperture diameter on the TBL noise inside a cavity, and finally the directivity evolution of a recessed microphone with the Mach number.

3.1 TBL noise assessment in cavity

In order to evaluate the acoustic signature and depth impact of a turbulent boundary layer (TBL), a Bruel and Kjaer type 4182 needle probe has been mounted on a millimeter movable screw behind a wiremesh. This assembly is mounted in a cylindrical cavity of 6mm depth and 15° aperture angle, as sketched on Fig. 14. The airtightness of the insert that is guiding the probe has been realized with dedicated seals, avoiding acoustic or aerodynamic leakages. Four Mach regimes have been investigated : 0.14,

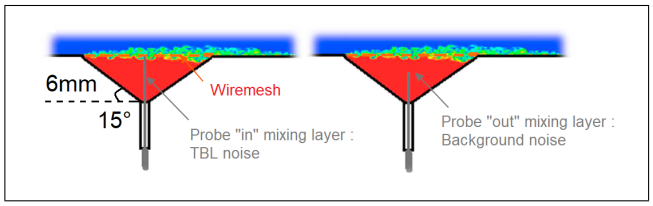

Figure 14. Sensor in (left) or out (right) of the mixing layer.

0.24, 0.40, and 0.56, leading respectively to average Mach of 0.1, 0.2, 0.3, and 0.45 . The twelve measured sensor positions relative to the wiremesh are (in mm) : 0, 0.5, 1, 1.5, 2, 2.5, 3, 3.5, 4, 5, 6, and finally 7.

Tab. 3 details the signal processing parameters used. Fig. 15 presents the sound pressure levels (SPL) of the

Span	40 kHz
Lines	1600
Δf	25 Hz
Window	Hann
Overlap	75 %
Averaging	20 s

Table 3. Autospectrum analysis parameters.

TBL noise inside the cavity (no acoustic excitation) . These values are extracted from narrow-band spectrum and normalized to the SPL measured when the sensor is in contact with the wiremesh, so at 0 mm. These results highlight

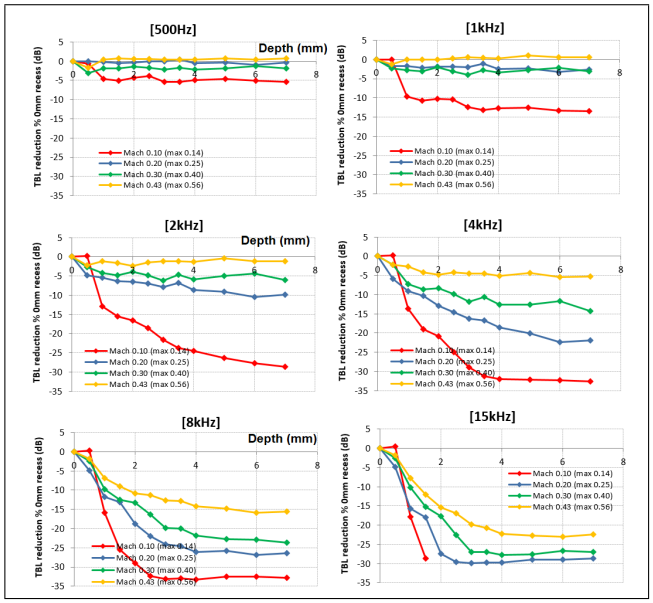

Figure 15. Normalized SPL of TBL noise in a wiremeshed cavity for several measurement depths.

that the TBL noise evolves very significantly in the first millimeters behind the mesh. It seems that the noise reduction function of the depth curves reaches an asymptote for high depths. When the probe is closed to the mesh, it is in the mixing layer and measures TBL noise (uncorrelated component), as sketched in Fig. 14 (right part). By comparing the different Mach numbers, it appears that the reduction is higher for lower Mach, which is directly linked to the background noise.

3.2 Impact of the cone angle on the TBL noise inside a cavity

At a given sensor recession depth, the shape and volume of the cavity might have an impact and therefore have to be assessed. For that, the needle probe is mounted as previously, travelling from the wiremesh contact back to a 7mm withdrawal. Fig. 16 presents the three geometries that have been characterized. They all consist of a tense wiremesh, a 6mm depth cavity, with 10, 12, and 15° aperture angles, and with their corresponding diameters, respectively 74, 63 and 51mm.

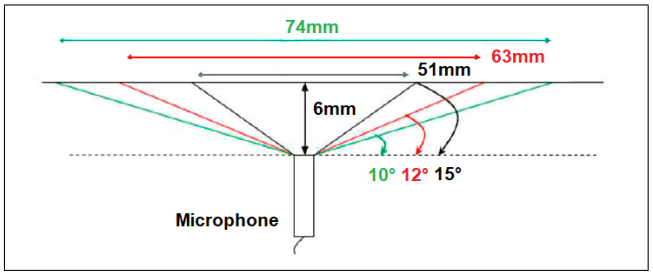

Figure 16. Sketch of the three cavity and cone designs.

Fig. 17 plots the reduction curves when compared to the position where the needle is in contact with the wiremesh, here for the 0.43 Mach number regime. The three cavities behave quite similarly over the frequency range, with the attenuation following the trend previously observed in Fig. 15. However, a significant discrepancy could be observed in the 15kHz frequency band, as highlighted in the orange area. After investigation, the wiremesh tightness is suspected. Indeed, this phenomenon happens for the largest diameter insert, and in such surface, it has been hard to master entirely the wiremesh installation. No tool or process to control the wiremesh tension has been used, as not being an usual requirement in the lab, where it is more common to bound the mesh over honeycomb cores for instance. This phenomenon is increasing in highest frequencies.

Apart a small unexpected event, no particular behavior has been observed in these investigations, with the aerodynamics only. This assessment will ease the measurement and analysis that will be performed with an additional acoustic excitation.

3.3 Impact of the Mach number on the directivity

One of the final purposes of such a test bench is to combine aerodynamics with acoustics. In order to evaluate the flow effect on the directivity of a given microphone mounting, a large test campaign has been carried out, including

- nine excitation frequencies : 500, 1k, 2k, 3k, 4k, 5k, 6k, 7k, up to 8k Hz,

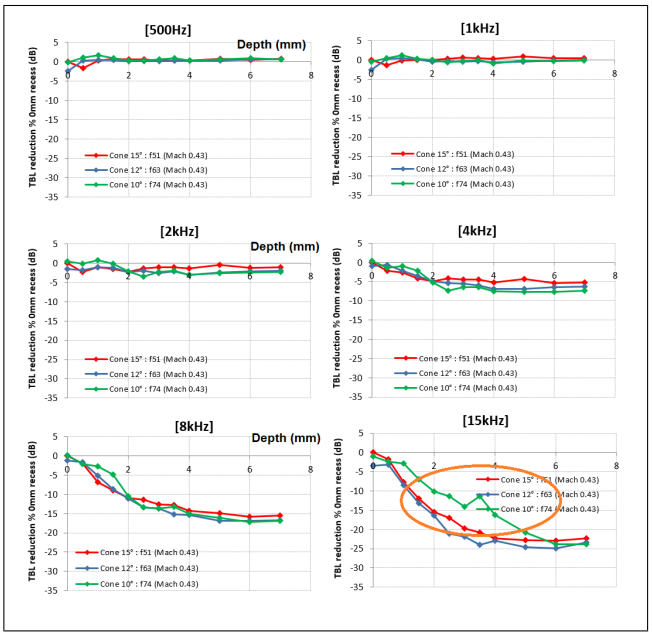

Figure 17. Normalized SPL of TBL noise for three cavities with wiremesh.

- five flow regimes with their Mach number as 0, 0.15, 0.26, 0.37, and 0.53,
- nine emission angles from 30, to 45, 62.1, 75.2, 90, 104.8, 117.9, 135, and up to 150°,

and this for the reference configuration, a 1/4 inch flush-mounted microphone, and for the cavity of interest, namely a 3mm-depth geometry with the same 1/4 inch microphone, with a 12° aperture angle and a conical profile, covered with a tense wiremesh.

To validate each test point of the 810 entries matrix, three criteria have been particularly monitored :

- the SPL difference between the flush and recessed microphones should be lower than 1dB, to ensure the repeatability (a control microphone is mounted in every generation horns),
- a SNR larger than 10dB, with the synchronous averaging presented previously in this paper,
- and a Mach number dispersion lower than 1%, so lower than 0.005 Mach difference at Mach 0.53 for instance.

The flow stream modifies the sound propagation and radiation patterns of the acoustic waves, mainly due to convection effects. As the BACCHUS bench lies in a comparative method, the propagation effects are assumed to be the same, as the propagation paths of flush and recessed microphones are almost the same in a given configuration. The propagation angle (incidence of the microphone) with convection effect can be calculated [11] from the geometrical propagation angle without flow such as Eqn. (8)

$$\Theta = \tan^{-1} \frac{\sin \Theta^{'}}{\cos \Theta^{'} - M} \tag{8}$$

where $\Theta^{'}$ is the source emission angle, and Θ is the propagation angle. Fig. 18 sketches the abovementioned situation. Fig. 19 plots the directivity diagrams relatively to

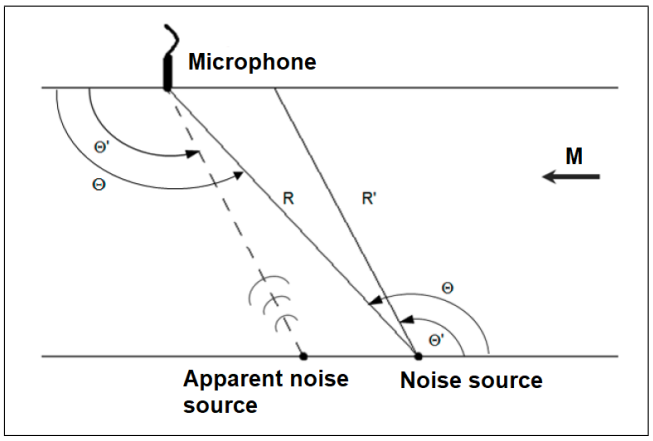

Figure 18. Sketch of the flow impact on the emission and propagation angles.

the reference, the 1/4 inch flush-mounted microphone. The values are normalized to 0 dB at 90°, after the wave convection correction. One can observe the elongation of the directivity lobes in the upstream direction. The higher the frequency, the higher the effect is. These findings on the directivity patterns movement are also very similar to the refraction effects of acoustic waves when crossing a turbulent boundary layer. In order to further understand such

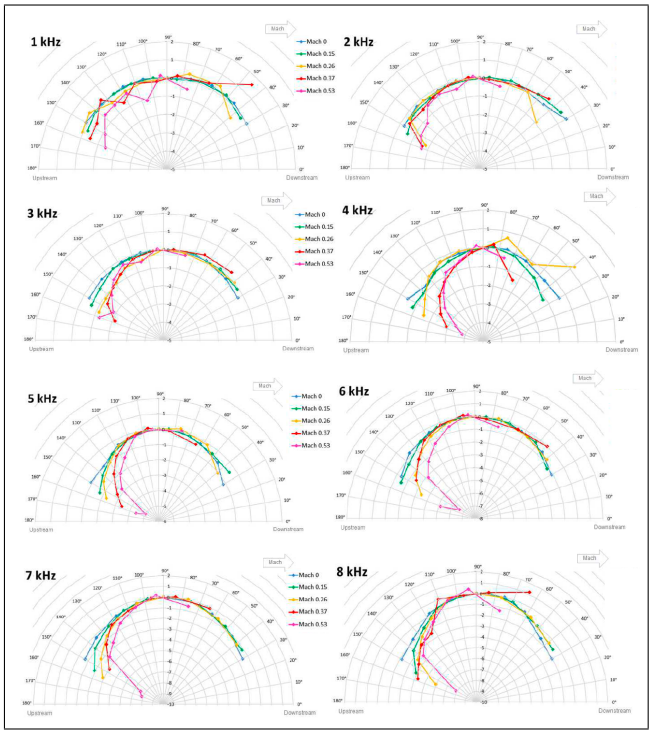

Figure 19. Mach number effect on the angular directivity of a cavity configuration.

behaviours, a more precise characterization of the boundary layer has to be performed on the upper wall of the anechoic vein (the microphone side), to correct the impact of

acoustic wave refraction on the receiving microphone incidence.

4. CONCLUSION

The BACCHUS bench has been presented in this paper, with some of its main features. This test rig has been developed to experiment both microphone assembly and de-noising method. For that, only three of the inner walls of the anechoic section are covered with absorbing foam, while the last one is rigid, allowing to imagine many sensor installations. The anechoicity characterization has been assessed not only at the foam level, but also to identify any unexpected reflection, as shown in the comparison between the bench as-is and with a rigid plate that blocks the bench on one side, using time auto-correlation analysis. The velocity profiles have been measured thanks to static pressure Pitot combs, and the roughness differences of the inner walls correspond to the obtained profiles.
Three test campaign outcomes are then presented, starting with an assessment of the mixing layer thickness into a conical cavity covered with wiremesh, by using a movable needle probe inside the cavity. The noise of the turbulent boundary layer evolves very significantly in the first millimetres behind the mesh, and putting the sensor out of this zone will largely improve the measurement. A second study has shown the limited impact of the angle of aperture (and associated diameter) at a given cavity depth in the case of pure aerodynamic excitation. However, this result will largely vary in the case of an acoustic excitation, mainly due to modal effect on the cavity. Finally, the angular directivity evolution of a given cavity configuration has been characterized thanks to a coupled aero-acoustic test campaign. The elongation of the directivity lobes tends to the upstream direction, and the higher the frequency, the larger is the effect. Such behaviours are quite similar to refractive effects of acoustic waves at turbulent boundary layer crossing.

The major benefit of the bench presented in this paper is its capacity to easily experiment different microphone mountings and post-processing methods, allowing to confront ideas to measured data, and with little resources, namely time and money. Indeed, as shown in the three studies performed, many configurations can be characterized, and the goal is to be able to perform dedicated parametric tests. The small technological bricks developed, once assembled together, can lead to unravel step by step the complexity of the aero-acoustic measurements.

5. REFERENCES

[1] S. Jaeger, W. Clifton Horne, and C. S. Allen, "Effect of surface treatment on array microphone self-noise," *AIAA Paper at 21st AIAA/CEAS*, 2000.

[2] V. Fleury, L. Coste, R. Davy, A. Mignosi, C. Cariou, and J. M. Prosper, "Optimization of microphone array wall mountings in closed-section wind tunnels," *AIAA Journal*, vol. 50, no. 11, pp. 2325–2335, 2012.

[3] F. Simon and D. Sebbane, "Caractérisation d'instrumentation en vue d'essais en souffleries - lot 2 : première simulation d'un montage wiremesh par éléments finis (first simulation of a wiremesh setup thanks to a finite element tool) [in french]," *ONERA report*, vol. 2/19557, 2013.

[4] F. Simon, N. Leclerc, and D. Sebbane, "Caractérisation d'instrumentation en vue d'essais en souffleries - lot 3 : résultats pour cinq montages de wiremesh en chambre anéchoique et en soufflerie basse vitesse (results for five wiremesh setup in an anechoic room and in a low-speed wind tunnel) [in french]," *ONERA report*, vol. 3/19557, 2013.

[5] D. Blacodon and J. Bulté, "De-reverberation of a closed test section of a wind tunnel with a multi microphones cepstral method," *Proc. Of Mtgs. Acoust.*, vol. 19, no. 055067, 2013.

[6] O. Saingès, "Noise measurements in turbulent boundary layers : Bacchus test bench validation," *Airbus report*, vol. M13022844, 2013.

[7] O. Saingès, "Noise measurements in turbulent boundary layers : aerodynamic characterization of bacchus test mean and assessment of recessed microphone fitting," *Airbus report*, vol. M1531359, 2015.

[8] A. Appel de Gardane, R. Pesseau, E. Julliard, A. Mosson, O. Saingès, and J. Derré, "Validation of numerical approach for assessing the performance of a microphone mounting in flow condition," *Forum Acusticum*, 2020.

[9] V. K. Madisetti, *The Digital Signal Processing Handbook*. CRC Press, 2nd ed., 2012.

[10] B. R. Munson, A. P. Rothmayer, T. H. Okiishi, and W. W. Huebsch, *Fundamentals of Fluid Mechanics*. Wiley, 7th ed., 2012.

[11] P. T. Soderman and C. S. Allen, *Microphone Measurements In and Out of Airstream*. Springer, 2002.